

Cite this: *Chem. Sci.*, 2018, 9, 2782

Structure and formation of highly luminescent protein-stabilized gold clusters†

D. M. Chevrier,^a V. D. Thanthirige,^{‡b} Z. Luo,^{‡c} S. Driscoll,^{‡a} P. Cho,^a M. A. MacDonald,^a Q. Yao,^c R. Guda,^b J. Xie,^c E. R. Johnson,^a A. Chatt,^a N. Zheng,^d and P. Zhang^{*a}

Highly luminescent gold clusters simultaneously synthesized and stabilized by protein molecules represent a remarkable category of nanoscale materials with promising applications in bionanotechnology as sensors. Nevertheless, the atomic structure and luminescence mechanism of these gold clusters are still unknown after several years of developments. Herein, we report findings on the structure, luminescence and biomolecular self-assembly of gold clusters stabilized by the large globular protein, bovine serum albumin. We highlight the surprising identification of interlocked gold-thiolate rings as the main gold structural unit. Importantly, such gold clusters are in a rigidified state within the protein scaffold, offering an explanation for their highly luminescent character. Combined free-standing cluster synthesis (without protecting protein scaffold) with rigidifying and un-rigidifying experiments, were designed to further verify the luminescence mechanism and gold atomic structure within the protein. Finally, the biomolecular self-assembly process of the protein-stabilized gold clusters was elucidated by time-dependent X-ray absorption spectroscopy measurements and density functional theory calculations.

Received 28th November 2017

Accepted 5th February 2018

DOI: 10.1039/c7sc05086k

rsc.li/chemical-science

Introduction

Composed of only tens or hundreds of Au atoms, Au clusters or nanoclusters (NCs) are highly stable 1–2 nm diameter particles with distinctive core/surface structures and molecule-like optical properties.^{1–4} Due to the high surface area and quantum confinement effects of Au NCs, stabilizing ligands often play an important role in directing their structure and properties. Besides small thiol molecules that are commonly used as protecting ligands for Au NCs, large and relatively more complex ligand types such as proteins and other biomolecules have been implemented to stabilize various sizes of Au particles, which further improves their integration into biological- and medical-related applications.^{5,6} Concurrently with the development of these new bionanomaterials, the biomolecular self-

assembly process that controls the formation of Au nanostructures has intrigued researchers for years.^{7–9}

Protein-stabilized Au NCs are a unique class of bionanomaterials with intense luminescence and highly specific chemical recognition properties suitable for biological imaging and chemical sensing applications.^{10–16} Conveniently, and rather remarkably, protein molecules can act as both the stabilizing ligand and the structure-directing agent to facilitate the formation of ultra-small Au clusters. This was successfully shown where highly luminescent Au NCs (quantum yield (QY) = ~6%, over 10⁸ times higher than bulk gold) were stabilized by bovine serum albumin (BSA) using a facile one-pot, protein-directed synthesis.¹⁷ This approach reduces the number of steps in Au NC synthesis and avoids the use of harsh chemical reagents, making it greener than general Au NC syntheses.

Despite the promising luminescence property of BSA-stabilized and other protein-stabilized Au NCs,^{18,19} little is known about the biomolecular self-assembly and atomic structure of Au NCs inside the protein. Complicating this unresolved puzzle are the reported inconsistencies on the relative Au(0)/Au(I) composition measured from X-ray photoelectron spectroscopy (XPS) and the disparity between Au_n/BSA compositions proposed from mass spectrometry (MS).^{13,20} To further complicate the problem, Au structure inside the BSA protein has been hypothesized to be Au₂₅(SR)₁₈ NCs^{21,22} even though they do not share similar photoluminescence or optical properties.

Identifying the atomic-level structure and self-assembled formation of Au NCs in the protein molecule would help

^aDepartment of Chemistry, Dalhousie University, 6274 Coburg Road, Halifax, NS, B3H4J3, Canada. E-mail: peng.zhang@dal.ca

^bDepartment of Chemistry, Western Michigan University, Kalamazoo, MI49008, USA

^cDepartment of Chemical and Biomolecular Engineering, National University of Singapore, 119260, Singapore

^dState Key Laboratory for Physical Chemistry of Solid Surfaces, Collaborative Innovation Center of Chemistry for Energy Materials, Engineering Research Center for Nano-Preparation Technology of Fujian Province, National Engineering Laboratory for Green Chemical Productions of Alcohols-Ethers-Esters, College of Chemistry and Chemical Engineering, Xiamen University, Xiamen, China

† Electronic supplementary information (ESI) available. See DOI: 10.1039/c7sc05086k

* Authors have made equal contributions.



determine the origin of protein-stabilized Au NC luminescence and lead to better-guided developments in sensing and imaging technologies. Experimental and investigative techniques beyond standard laboratory methods (*e.g.*, FT-IR, XPS, MS) were applied in order to reveal more informative and reliable details on Au NC structure and properties. Synchrotron-based X-ray absorption fine structure (XAFS) spectroscopy was critical in this regard, as it provided the ability to resolve interactions between few-atom Au clusters and stabilizing protein residues from an element-specific perspective. In conjunction with other experimental techniques and in-depth analyses, the atomic structure of Au in BSA was surprisingly found to resemble interlocked gold-thiolate (Au-SR) ring structures, which slowly develop over the course of the protein-directed synthesis. Additional experiments and quantum calculations are presented that consistently support the atomic structure of Au in BSA. The distinctive red luminescence property, as it relates to the newly identified structure, is also examined.

Results and discussion

Structure of protein-stabilized gold clusters

The synthesis of red luminescent BSA-stabilized Au clusters (AuBSA) is schematically shown in Fig. 1. This facile, protein-directed protocol employs amino acid residues of the protein to interact and control the formation of Au clusters. In alkaline solution conditions and with the right concentration of BSA and Au(III) precursors, red luminescent Au clusters are formed (Fig. S1†).¹⁷ Our initial investigation utilized extended-XAFS (EXAFS) to determine whether Au structures in AuBSA are related to the core/shell structures of atomically precise NCs, such as Au₂₅(SR)₁₈, which reports on protein-stabilized Au NCs have suggested.^{13,20} The extended region of the Au XAFS spectrum provides local structural information for Au atoms stabilized by the protein. The scattering features observed in the Fourier transform of the EXAFS spectrum (FT-EXAFS) can be linked to specific bonding environments, either qualitatively compared with reference materials or quantitatively refined



Fig. 1 One-pot protocol for the synthesis of protein (bovine serum albumin)-stabilized luminescent Au clusters.



Fig. 2 Structural identification of AuBSA clusters. (A) Au L₃-edge FT-EXAFS of luminescent AuBSA (black line) with Au₂₅(SR)₁₈ (red dot) and Au₃₈(SR)₂₄ (blue dot) (inset, respective models with Au (yellow) and S (red) atoms). (B) Simulated Au L₃-edge FT-EXAFS of Au(I)-SR structures (i) Au₄S₄ ring, (ii) Au₅S₅ ring, (iii) Au₆S₆ ring, (iv) Au₁₀S₁₀ catenane, (v) Au₁₁S₁₁ catenane, (vi) Au₁₂S₁₂ catenane and (vii) Au-S double helix (methyl substituents were omitted from all structures for clarity). (C) Models of Au(I)-SR structures and 4 representative EXAFS scattering paths from the Au₁₀(SR)₁₀ catenane model used for fitting (a – inter-ring and b – intra-ring). (D) Au L₃-edge FT-EXAFS of Au₁₀(SG)₁₀ (SG – glutathione) and AuBSA.

with a fitting analysis. Fig. 2A directly compares the FT-EXAFS of luminescent AuBSA with Au₂₅(SR)₁₈ and Au₃₈(SR)₂₄. The spectral regions corresponding to Au-S and Au-Au bonding are highlighted in blue and orange, respectively. The overlap of each reference FT-EXAFS spectrum with AuBSA clearly shows there is no significant Au core structure, as evidenced by the absence of metallic Au-Au scattering in the 2.5–3.0 Å region. Fitting the Au-S region of AuBSA EXAFS (Table S1, Fig. S2†) yielded a coordination number (CN) of 2.1(1) and a bond length of 2.31(2) Å. Thus, most Au atoms are in RS-Au-SR structures (CN = 2 and SR – cysteine from BSA) with no Au core structure, meaning an oxidation state of Au(I) is expected for Au atoms in AuBSA. This is substantiated by inspection of the X-ray absorption near-edge structure (XANES) region of AuBSA with Au(I) and Au(0) reference materials (Fig. S3†). From this initial result, the AuBSA system appears to be better classified as a Au(I)-SR cluster or complex rather than a Au NC with core/shell architecture.

Although Au-Au scattering representing Au core structures was not found in the EXAFS fitting of AuBSA, longer-range Au-



utilized to identify physical characteristics that are unique to AuBSA clusters, despite having the same Au cluster structure.

AuBSA have PL centered at 650 nm when excited at 365 nm (Fig. S9†). The excitation spectrum shows that two peaks, one at 365 nm and another at 475 nm, are responsible for the observed luminescence. The QY was determined to be 6.8% (photo-physical results are shown in Table S4†). The large Stokes shift (285 nm) and long PL decay lifetime (1.065 μ s, Table S4†) further suggest the emission from AuBSA clusters is characteristic of phosphorescence, similar to other known Au(I)-SR structures.^{37,38}

Although a virtually-identical Au local structure was determined from our EXAFS analysis, Au₁₀(SG)₁₀ shows a modest difference in emission energy, centered at 620 nm (excitation at 365 nm) instead of 650 nm, but more importantly, a significantly weaker emission intensity (Fig. S9†) with a QY of only 0.48%. The second excitation peak at 475 nm appears as a shoulder instead of a strong peak as seen for AuBSA clusters. This could indicate the larger protecting protein increases the oscillator strength of the electronic transition at this particular energy. The small discrepancy in maximum emission energy between AuBSA and Au₁₀(SG)₁₀ (\sim 0.09 eV) can be attributed to the difference in ligand type (protein *versus* tripeptide) having varied electron withdrawing ability.³⁹ If there are inter-cluster interactions between Au(I)-SR structures in AuBSA clusters, this could also further red-shift the emission from orbital splitting.³⁷ With regards to the substantial difference in QY however, the larger encapsulating BSA protein could prevent photo-excited energy loss between Au(I)-SR ring structures and the surroundings. To test the importance of the protecting protein for the enhanced luminescence, the encapsulating protein shell protecting Au(I)-SR clusters was disrupted *via* enzymatic digestion with trypsin (schematically shown in Fig. 3A). After cleaving BSA molecules with trypsin digestion, the local structure of Au(I)-SR clusters remained mainly intact as shown by Au L₃-edge EXAFS (Fig. S10†), but the PL intensity had decreased \sim 5 fold (Fig. 3B) and emission maximum red-shifted by 15 nm.

The loss of the hierarchical protein structure from enzyme digestion may also affect the structural rigidity of Au(I)-SR clusters, a physical property of thiolate-stabilized Au NCs and other systems that has been recently reported to facilitate efficient emission release.^{40–42} This is related to protein-stabilized Au clusters since cysteine residues from BSA that bond with Au are fixed to the protein backbone, which could provide the aforementioned structural rigidity of Au(I)-SR clusters within BSA. This would further enable stronger auophilic interactions between interlocking Au(I)-SR ring structures, inducing ligand to metal–metal charge transfer (LMMCT), an effect known to cause or enhance luminescence for Au(I) oligomers and complexes.^{38,41,43–45}

In order to emulate the emission properties of AuBSA clusters with Au₁₀(SG)₁₀, the protecting and rigidifying environment of the protein was mimicked by performing a water/toluene phase-transfer experiment^{44,46} with Au₁₀(SG)₁₀ (Fig. S11,† experimental details found in Materials and methods). Tetraoctylammonium (TOA⁺) ions act as phase-transfer agents, which bring Au₁₀(SG)₁₀ clusters into the organic-phase *via* electrostatic interaction between ammonium (NR₄⁺) and carboxylic end groups (COO⁻)

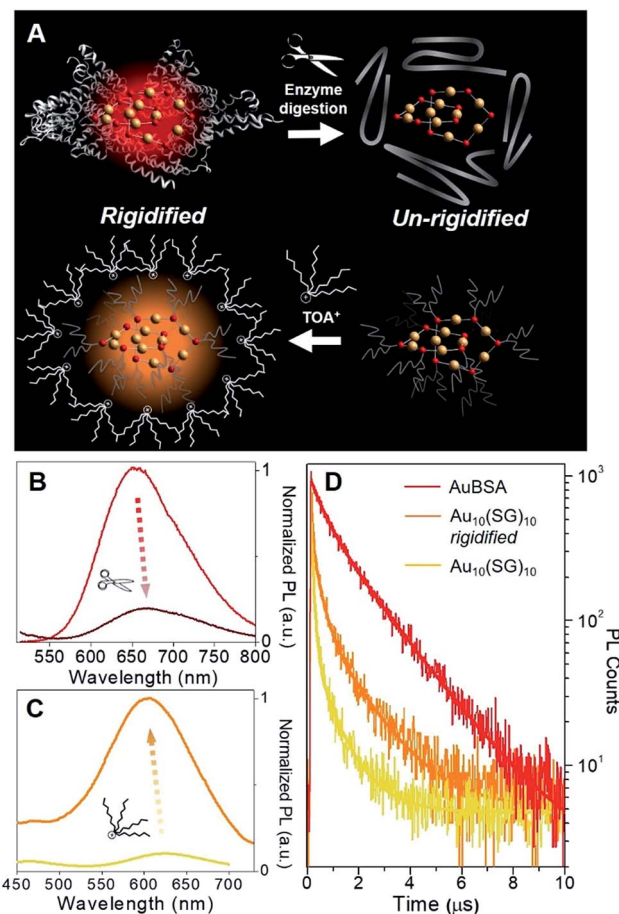


Fig. 3 Photoluminescence properties of Au₁₀(SG)₁₀ and AuBSA clusters in rigidified and un-rigidified states. (A) Scheme of un-rigidifying AuBSA clusters with enzyme digestion and rigidifying Au₁₀(SG)₁₀ clusters with TOA⁺/toluene phase-transfer. (B) Resultant luminescence decrease of AuBSA clusters (un-rigidified, dark red line) and (C) luminescence enhancement of Au₁₀(SG)₁₀ clusters (rigidified, orange line). (D) Photoluminescence decay lifetime traces of AuBSA clusters (red), rigidified Au₁₀(SG)₁₀ clusters (orange) and original Au₁₀(SG)₁₀ clusters (yellow).

of SG ligands. The aliphatic octyl chains from TOA⁺ protect and isolate Au₁₀(SG)₁₀ clusters from the solvent environment and restrict molecular vibrations or rotations of the SG ligands (Fig. 3A, bottom), thereby creating a “rigidified” state.

The luminescence of rigidified Au₁₀(SG)₁₀ was enhanced by > 10 fold (QY = 5.0%) with a blue-shift of 15 nm (620 nm \rightarrow 605 nm, see Fig. 3C). The 15 nm blue-shift observed here is in line with the 15 nm red-shift seen above in the opposite direction for AuBSA (Fig. 3B), further verifying a similar rigidifying effect on the Au(I)-SR clusters. The average PL decay lifetime for rigidified Au₁₀(SG)₁₀ had also nearly doubled (from 0.120 to 0.210 μ s, Fig. 3D and Table S4†). Together, increased PL lifetime and enhanced QY point to a rigidified state created for Au₁₀(SG)₁₀ clusters. Rigidifying Au₁₀(SG)₁₀ and un-rigidifying Au(I)-SR clusters in BSA demonstrate the similar luminescence property that exists in these two systems, further linking the luminescence properties of small thiolate-stabilized Au NCs with the new category of protein-stabilized Au clusters.



Protein-directed self-assembly of gold clusters

Following the identification of interlocked Au(I)-SR ring structures, the biomolecular self-assembly process guided by BSA could then be further understood by monitoring the protein-directed synthesis with a time-dependent XAFS study. Samples at 0, 1, 2, 3, 6, and 12 h were extracted from the synthesis to capture two distinct stages of the protein-directed synthesis, including an ion-exchange involving the Au(III) precursor. Photoluminescence, Au L₃-edge XANES and EXAFS spectra were collected for samples at each time point indicated above and are presented in Fig. 4A, B and 5A, respectively (absorbance and *k*-space of each sample shown in Fig. S12 and S13,† respectively).

Photoluminescence increased steadily over the course of the protein-directed synthesis until 12 h. Even after 36 h, the photoluminescence intensity did not increase further (Fig. S14†). Au L₃-edge XANES spectra in Fig. 4B show the white-line intensity (*i.e.*, first feature that follows the absorption edge, and the intensity of this feature reflects the valence electron occupancy, which is mainly the 5d level for Au at the L₃-edge) decreased over the course of the synthesis, which signified a reduction of Au(III) precursor to Au(I)-SR clusters. A white-line valence state integration analysis (inset, Fig. 4B) reveals no further reduction of Au(I) after 6 h into the synthesis. S K-edge XANES spectra were also collected for each sample to detect structural changes to the protein through cleavage of disulfide bonds (Fig. S15†). Near-edge features decrease in intensity and change in spectral appearance (relative intensity of two main features at 2472 and 2473 eV) over the course of the protein-directed synthesis. From pristine BSA (mainly disulfide) to time-dependent AuBSA samples, the S K-edge XANES indicate disulfide bonds are disrupted over 12 h to accommodate bonds with Au atoms, resulting in a final XANES spectrum at 12 h that resembles cysteine and Au(I)-SR references.

Using Au-X EXAFS scattering paths (where X is Cl, O, S or Au), quantitative structural parameters were determined by fitting the time-dependent Au L₃-edge EXAFS spectra (Fig. 5A and Table S5†). A time plot of Au-X CN parameters is shown in Fig. 5C to convey a two-stage process (0–3 h and 3–12 h). The first scattering path at ~1.7 Å (spectra not phase corrected) for

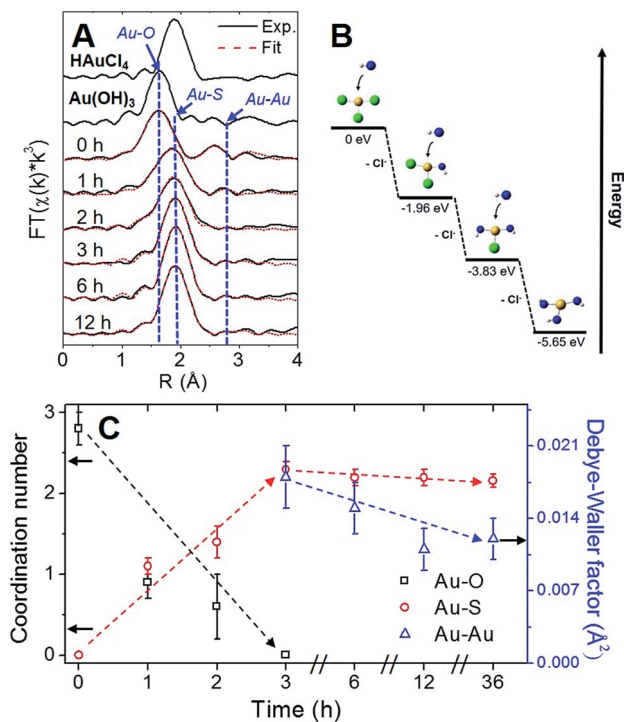


Fig. 5 (A) Au L₃-edge FT-EXAFS with fitted spectra and reference materials. (B) Relative DFT energies of AuCl₃ (set to 0 eV), Au(OH)₃, and intermediate products of the precursor ion-exchange process. (C) Coordination and Debye–Waller (Au–Au shell only) plot for time-dependent EXAFS fitting results.

the 0 h spectrum in Fig. 5A was determined from EXAFS fitting to be Au–O bonding at 2.02(1) Å and surprisingly not Au–Cl bonding from the Au(III) precursor (HAuCl₄). A comparison with HAuCl₄ (starting material) and Au(OH)₃ reference compounds is shown above the 0 h sample in Fig. 5A to further demonstrate the similarity to the latter reference. EXAFS fitting of Au–O scattering for Au(OH)₃ gave a bond length of 2.005(4) Å (Fig. S16†), similar to the 0 h sample. DFT calculations support the transformation of gold chloride to gold hydroxide in the presence of excess OH[−] ions (Tables S6–S8†). The formation energy was calculated for each step of the ion-exchange reaction with each intermediate chlorohydroxoaurate complex, shown in Fig. 5B. It was found that the formation of Au(OH)₃ from AuCl₃ has a total formation energy of −5.65 eV with the energies of the ion-exchange steps ranging from −1.82 to −1.96 eV. With excess NaOH present, elevated temperatures and vigorous mixing in the protein-directed synthesis of AuBSA clusters, the initial formation of Au(OH)₃ is highly favourable.

After 1 h into the synthesis, Au–S bonding appears (feature at ~2 Å in Fig. 5A) with an EXAFS fitted distance of 2.31(1) Å. At this point in the synthesis, Au atoms begin to form strong covalent bonds with cysteine residues in BSA, which were originally bonded to other cysteine residues *via* disulfide bonds. The nature of the Au–S bonding does not change from 3 h until the end of the synthesis, with an average bond distance of 2.32(1) Å and a CN of 2.1(1). Notably, appreciable luminescence is first observed around 3 h (Fig. 4A), which is the point where SR-Au(I)-SR structures have mainly formed with no remaining



Fig. 4 (A) Photoluminescence spectra (excitation $\lambda = 470$ nm) and (B) Au L₃-edge XANES (inset, white-line integration analysis for Au(III) to Au(I) formation) following the course of the protein-directed assembly of Au clusters.



Au–O interactions. The complete ligand-exchange (hydroxide to cysteine) and formation of SR-Au(I)-SR structures from 0–3 h can be regarded as Stage I of the protein-directed synthesis.

Stage II of the protein-directed synthesis is the optimization or final assembly of SR-Au(I)-SR structures. Au–Au interactions were resolvable from EXAFS spectra for samples 3, 6, and 12 h, with a consistent bond distance around 3.02 Å and a CN parameter decreasing from *ca.* 2 to 1 (Table S5†), which is suggestive of inter-ring Au–Au interactions early on in Stage II. From 3 to 12 h, the Debye–Waller factor (σ^2 , accounts for thermal and positional disorder of neighbouring atoms in a particular scattering shell) and associated error value decreases for inter-ring aurophilic interactions (plotted in Fig. 5C, right y-axis), indicating that Au(I)-SR clusters are becoming more ordered inside of the protein as incubation and mixing progresses. Since the change in Au local structure is minimal from 3 to 12 h, the increase in luminescence during this stage could be due to the structural optimization of BSA to accommodate the formed Au(I)-SR interlocking ring structures within the protein. No further change in Au local structure was observed even after 36 h of incubation and mixing (Fig. S17 and Table S5†).

Conclusions

This work has elucidated the structure of highly luminescent gold nanoclusters stabilized by bovine serum albumin. Using a multi-step procedure that included screening of gold-thiolate model structures, experimental and simulated X-ray absorption spectroscopy, analogous free-standing gold nanocluster synthesis and rigidifying/un-rigidifying experiments, the structure of the bioinorganic nanoclusters was revealed along with the structural origin of their luminescence property and biomolecular self-assembly mechanism. These findings accentuate the remarkable capability of a protein nano-reactor for producing bioinorganic clusters with intriguing structures and luminescence properties, and should be of importance for future preparation and application of luminescent protein-gold bionanomaterials. The investigative approach demonstrated in this work could also be extended to other biomolecule-metal materials where a large biological system interferes with characterization of the encapsulated metal component.

Materials and Methods

Chemicals

HAuCl₄·3H₂O (Alfa Aesar, 99.99% metal basis), bovine serum albumin (BSA) (Sigma Aldrich, ≥96% purity), NaOH (ACP Chemicals, ≥97.0% purity), tetraoctylammonium bromide (TOABr, 98%), toluene (ACS grade), nanopure water (Barnstead millipore system, 18.2 MΩ cm), dialysis tubing (Fisherbrand, 12 000–14 000 MWCO).

Protein-directed synthesis of Au clusters

AuBSA were synthesized following a procedure from Xie *et al.*¹⁷ A 5 mL aqueous solution of bovine serum albumin (50 mg mL⁻¹) was incubated at 37 °C with vigorous mixing. Once BSA

dissolved (5 min), a 5 mL aqueous solution of HAuCl₄·3H₂O (10 mM) was added to the reaction vessel containing BSA. 500 μL of a 1 M NaOH solution was added to the reaction 2 min later, raising the pH of solution to ~11–12. The reaction proceeded with incubation at 37 °C and stirring for at least 12 h. Nanopure water (18.2 MΩ cm) was used to make up all solutions for the synthesis. For the time-dependent study, samples were taken at 0, 1, 2, 3, 6, 12 and 36 h from the reaction, immediately frozen and then lyophilized for further studies (0 h sample was taken as soon as NaOH was added to the reaction). Luminescence was preserved after the lyophilisation (Fig. S1†). Samples measured for multi-shell EXAFS fitting were dialyzed against nanopure water (18.2 MΩ cm) for 24 h with fresh nanopure water changed every 8 h. For destabilizing AuBSA *via* enzymatic digestion, 0.5 mL of a freshly prepared 0.1 mg mL⁻¹ trypsin solution was added to 1 mL of the purified AuBSA. This solution was mixed and incubated for 1 day.

Au(I)-SC₁₂H₂₅ polymer synthesis (Au(I) reference)

This synthesis closely follows a protocol by Cha *et al.*⁴⁷ Briefly, a 0.1 M tetrahydrofuran (THF) solution of *n*-dodecanethiol was added to a 0.02 M THF solution of HAuCl₄·3H₂O of equal volume. The mixture was stirred for 1 day and a white precipitate was formed. This was collected as the product, which was washed and dried under vacuum before XAFS measurement.

Au₁₀(SG)₁₀ synthesis

In a typical synthesis, GSH (0.1 M, 0.20 mL) was mixed with 4.30 mL of nanopure water, followed by the addition of HAuCl₄·3H₂O (0.02 M, 0.50 mL) under gentle stirring (500 rpm) at 25 °C for 5 min. A precipitate was formed, which was then dissolved by adjusting pH to ~7 with NaOH (0.5 M). The solution was aged for 2 h at 40 °C, and the resultant solution of oligomeric Au(I)-thiolate complexes was lyophilized without purification for further characterizations.⁴⁴

Au₁₀(SG)₁₀ rigidification studies

In a typical procedure, 10 mg of Au₁₀(SG)₁₀ dissolved in 10 mL of nanopure water and 10 mg of TOABr dissolved in 5 mL of toluene were added together into a 20 mL scintillation vial. The pH of aqueous solution was then adjusted to pH 9.0 by adding NaOH to ensure carboxyl groups of glutathione were in the anionic form. The electrostatic interaction between the carboxylate anions of the glutathione ligand and the hydrophobic TOA cations in the toluene phase is strong, therefore the TOA⁺-paired Au₁₀(SG)₁₀ clusters can be readily transferred to the toluene phase (referred to as the “rigidified” state) by stirring the two solutions. The toluene phase was then separated and washed with copious amounts of water to wash away all the water-soluble impurities.

Absorption and photoluminescence of AuBSA

UV-Vis and fluorescence spectroscopy measurements for the time-dependent study another supporting measurements besides the rigidifying experiments were collected with the Cary



